IOP Conf. Series: Journal of Physics: Conf. Series **1224** (2019) 012021 doi:10.1088/1742-6596/1224/1/012021

Design and commissioning of an experimental facility for performance evaluation of pure and mixed refrigerants

Luca Molinaroli, Andrea Lucchini, Luigi Pietro Maria Colombo

Dipartimento di Energia, Politecnico di Milano, via Raffaele Lambruschini 4/A, 20156, Milano (MI), Italy

E-mail: luca.molinaroli@polimi.it

Abstract. The recent regulations about fluorinated greenhouse gases introduce a rapid phase-down of traditional, environmentally harmful refrigerants. Consequently, new working fluids are continuously appearing on the market, leading to the need of testing them to analyse their performance before making an ultimate choice. In the present paper, a test rig built to carry out experimental studies on different refrigerant in a drop-in application is described and first results for the set-up commissioning are commented. The experimental campaign was carried out in typical water-to-water heat pump operating conditions, varying the cold water temperature at evaporator inlet from 10 °C to 20 °C, with a step of 2.5 °C, and hot water temperature at condenser inlet from 30 °C to 50 °C, with a step of 10 °C and the compressor shaft rotational frequency from 30 Hz to 80 Hz, with a step of 10 Hz. The first findings demonstrate that the experimental results of some key performance parameters, namely heating capacity, COP and compressor volumetric efficiency, agree well with open literature trends, allowing to state that the experimental facility was correctly designed and can be used to deep the analysis on performance assessment of new refrigerants in a drop-in application.

1. Introduction

The recent EU 517/2014 regulation [1] and the Kigali amendment [2], force the air conditioning and refrigeration industry to find new refrigerants able to cope with more and more severe limits on Global Warning Potential (GWP). As a consequence, in the last years new refrigerants have been continuously introduced and the need of testing them in vapour compression systems to analyse their performance arises.

For example, the substitution of the largely used working fluid in refrigeration applications, R404A, was studied both from a theoretical point of view [3] and from an experimental point of view [4] with low GWP refrigerants and, similarly, the replacement of refrigerants traditionally used in air conditioning and heat pump applications, namely R410A for small to medium capacity systems and R134a for medium to large capacity systems, with new, low GWP alternatives was analysed by several authors considering both natural [5] and synthetic refrigerants [6, 7, 8]. The general findings of these wide screening of several alternatives were that the energy efficiency of system using the new refrigerants could achieve the same value of the traditional refrigerant-based based systems, but an adjustment of expansion device, charge and, above all, compressor swept volume are required.

In this framework, the experimental analysis of the performance of systems that use new refrigerants is of primary importance since it could provide not only data about the system operation with a new working fluid but also an useful feed-back for system adjustment or re-design. Therefore, the goal of the present paper is to describe a test rig recently built to carry out experimental studies on different refrigerants in a drop-in application. The experimental set-up mimics a water-to-water system equipped with variable speed compressor and fully instrumented to measure and acquire all the relevant parameters.

2. Experimental methodology

2.1. Experimental set-up

The layout of the experimental set-up used to assess the refrigerant performance is shown in Figure 1. The test rig mimics a water-to-water system and consists of three different loops:

(i) The first loop is the refrigerant loop, whose main components are a semi-hermetic, variable speed, reciprocating compressor, two stainless steel plate heat exchangers (i.e. the condenser and the evaporator) and two electronic expansion valves (in parallel). This loop was used to reach the desired refrigerant mass flow rate and superheating at evaporator outlet acting on the compressor shaft rotational frequency and on the expansion valve set-point respectively.

(ii) The second loop is the cold water loop and mainly consists of a variable speed pump, a thermal storage and a three-way valve. This loop was used to set the water mass flow rate and temperature at evaporator inlet to the desired values whereas the thermal storage allows to reduce the water temperature fluctuations and to reach stable testing conditions.

(iii) The third loop is the hot water loop and is built considering the same components found in the previous one and adding an auxiliary chiller. This loop was used to set the water mass flow rate and temperature at condenser inlet to the desired values and to reach stable operating conditions thanks to the thermal storage.

The main characteristics of the test rig components are provided in Table 1

Table 1. Main characteristics of the experimental set-up components.

Component	Parameter	Range
Compressor	Swept volume @ 50 Hz	13.15 $m^3 \cdot h^{-1}$
	Shaft frequency	30 Hz - 87 Hz
Condenser	Height x Width x Depth	289 mm x 119 mm x 93.6 mm
	No of plates	40
Evaporator	Height x Width x Depth	376 mm x 119 mm x 71.2 mm
	No of plates	30
Expansion valve	Capacity range	1200 W - 12000 W
	Capacity range	1690 W - 16900 W
Liquid receiver	Volume	$2.8 \cdot 10^{-3}$ m^3
Suction accumulator	Volume	$2.33 \cdot 10^{-3}$ m^3
Oil separator	Volume	$2.8 \cdot 10^{-3}$ m^3
Recuperator	Height x Width x Depth	193 mm x 76 mm x 71.2 mm
	No of plates	30

The water-to-water unit was charged under Group 1 reference condition (see Table 3) considering a superheating at evaporator outlet equal to 5 K and a subcooling at condenser outlet equal to 3 K as target values. The final charge of R134a was 4 kg.

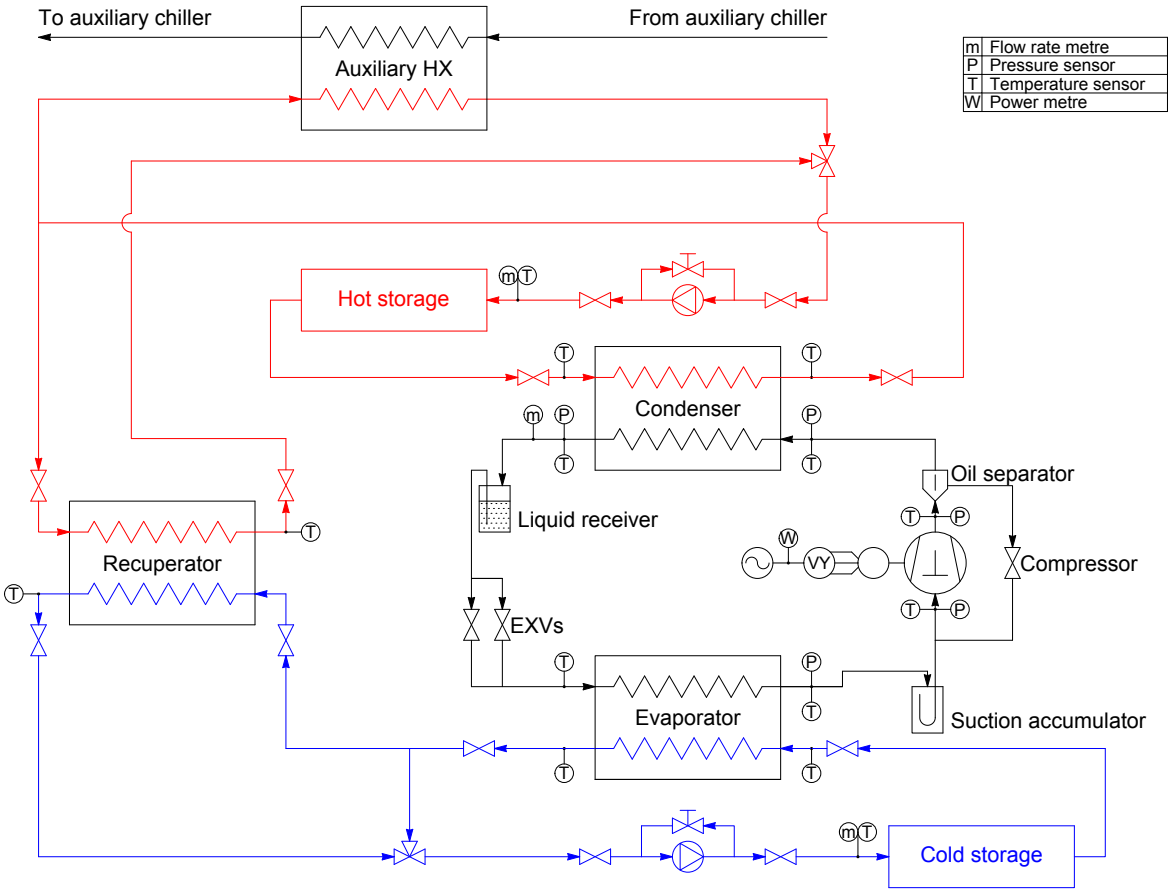

Figure 1. Schematic of the experimental set-up.

The test rig was equipped with instrumentations that allow for the data acquisition of the main parameters such as pressures, temperatures, flow rates and power. The positions of all the measurement devices are shown in Figure 1 while their main characteristics are collected in Table 2 where, for the sake of completeness, it is worth specifying that the water mass flow metre is equipped also with a RTD Pt 1000 temperature probe whose accuracy is equal to 0.1 K.

2.2. Experimental procedure

The following experimental procedure was adopted to run each test:

(i) The cold and hot water pumps are switched on and the RPM are set to the values needed to guarantee the water mass flow rates required by the test.

(ii) The compressor is switched on and the shaft rotational frequency is set to the value required by the test.

(iii) The cold and hot water temperatures required by the test are set at the inlet of the two tanks acting on the 3-way valves. Consequently, the water temperature inside both tanks slowly changes as a result of the mixing process and the same happens to the water temperature at evaporator and condenser inlets.

Table 2. Measurement instrumentation and accuracy.

Parameter	Instrument	Range	Accuracy
Refrigerant mass flow rate	Coriolis mass flow metre	0 kg·h^{-1} - 300 kg·h^{-1}	±0.15% r.v.
Refrigerant pressure	Pressure transducer	0 kPa - 4000 kPa	±0.3% f.s.
Refrigerant temperature	RTD Pt 100	243.15 K - 343.15 K	±0.1 K
Water mass flow rate	Vortex flow metre	0.21 m^3·h^{-1} - 3 m^3·h^{-1}	±2% r.v.
Water temperature	RTD Pt 100	253.15 K - 353.15 K	±0.1 K
Compressor power	Power transducer	0 W - 4000 W	±0.2% f.s.

(iv) Once the water temperature at evaporator and condenser inlet has reached the value required by the test, the data acquisition starts with a sample rate equal to 1 s. For each of the measured pressures and temperatures (see Fig. 1), the simple moving average is calculated considering the last 900 samples.

(v) If the deviation of each measured pressure and temperature lies within ± 10 kPa and ± 0.2 K respectively, the test is considered in steady-state condition and further 900 samples are recorded for data analysis.

(vi) Finally, at the end of the test, the evaporator and condenser capacities are calculated based on both the water temperatures and refrigerant enthalpies. If the values agree within ± 4% the experimental test is considered completed otherwise it is repeated.

2.3. Data reduction

The water-to-water system was operated as if it was a heat pump, therefore the condenser capacity is the useful effect and the performance index is the COP.

The condenser capacity, $\dot{Q}_{COND}$, was determined as the average between the refrigerant-side value and the water-side value according to the following equation:

$$\dot{Q}_{COND} = \frac{1}{2}\left[\dot{m}_R\left(h_{R,IN,COND} - h_{R,OUT,COND}\right) + \dot{m}_W c_{P,W}\left(T_{W,OUT,COND} - T_{W,IN,COND}\right)\right] \tag{1}$$

REFPROP [9] software was used to calculate the water isobaric heating capacity, as function of water temperature, and the refrigerant enthalpies, as function of refrigerant pressure and temperature.

The coefficient of performance, COP, was calculated neglecting the power consumption of the two pumps and the power consumption of the EXV controller as follows:

$$COP = \frac{\dot{Q}_{COND}}{\dot{W}_{COMP}} \tag{2}$$

where, it is worth specifying, the compressor power, $\dot{W}_{COMP}$, accounts also for inverter losses.

Finally, the volumetric efficiency, η_{VOL}, of the compressor is defined as the ratio between the actual, $\dot{v}_{ACT}$, and the maximum theoretical, $\dot{v}_{THE}$, volume flow rate at compressor suction:

$$\eta_{VOL} = \frac{\dot{v}_{ACT}}{\dot{v}_{THE}} = \frac{\left(\dot{m}_R/\rho_{R,IN,COMP}\right)}{V_{COMP} f_{ROT,COMP}} \tag{3}$$

where the density of the refrigerant at suction pressure and temperature, $\rho_{R,IN,COMP}$, is again calculated using REFPROP [9] software.

2.4. Uncertainty analysis

The uncertainty of all the quantities, both directly measured and calculated, was estimated according to Moffat [10]. More in detail, the experimental uncertainty u_x of each directly measured variable x was calculated as follows:

$$u_x = \pm\sqrt{u_{x_{INST}}^2 + (t_{95}\sigma_{\overline{x}})^2} \tag{4}$$

where $u_{x_{INST}}$ is the instrumental uncertainty of the directly measured variable, t_{95} is the Student test multiplier at 95% confidence level and $\sigma_{\overline{x}}$ is the standard deviation of the mean value of the collected samples.

Similarly, the uncertainty u_y of the generic calculated quantity y was estimated using the combined standard uncertainty under the uncorrelated input quantities assumption:

$$u_y = \pm\sqrt{\sum_{i=1}^{N}\left(\frac{\partial y}{\partial x_i}u_{x_{INST}}\right)^2 + t_{95}^2\sum_{i=1}^{N}\left(\frac{\partial y}{\partial x_i}\sigma_{\overline{x_i}}\right)^2} \tag{5}$$

being N the number of uncorrelated input quantities y depends on.

3. Results

The commissioning of the experimental set-up was carried out through a set of experimental tests. Tests were organized in 4 groups that were chosen to assess the influence of the water temperature at evaporator inlet, of the water temperature at condenser inlet and of the rotational frequency of compressor shaft on system performance. The test conditions used in the experimental campaign are reported in Table 3. In the same table, the bold values shown for each group represent the values of the experimental conditions used to find the evaporator and condenser water flow rates that lead to a temperature difference across them equal to 5 K.

Table 3. Testing conditions (bold values are the reference values).

Group No	$f_{ROT,COMP}$ [Hz]	$T_{W,IN,EVAP}$ [°C]	$T_{W,IN,COND}$ [°C]
1	50	10, 12.5, **15**, 17.5, 20	30
2	50	10, 12.5, **15**, 17.5, 20	40
3	50	10, 12.5, **15**, 17.5, 20	50
4	30, 40, **50**, 60, 70	10	30

All tests where run acting on the EXV so that the target superheating was 5 K in stable working conditions.

The condenser heating capacity and the system COP found under groups No 1, 2 and 3 testing conditions (see Table 3) are shown in Fig. 2 and in Fig. 3 respectively. For each water temperature at condenser inlet, the heating capacity shows an increasing trend with the water temperature at evaporator inlet while the heating capacity reduces as the water temperature at condenser inlet increases with the same water temperature at evaporator inlet. This trend is justified considering that the higher the water temperature at evaporator inlet, the higher the

evaporating temperature and pressure which, in turn, leads to a higher refrigerant density at compressor inlet. When the suction density gets higher, the refrigerant mass flow rate increases and, consequently, the capacity increases.

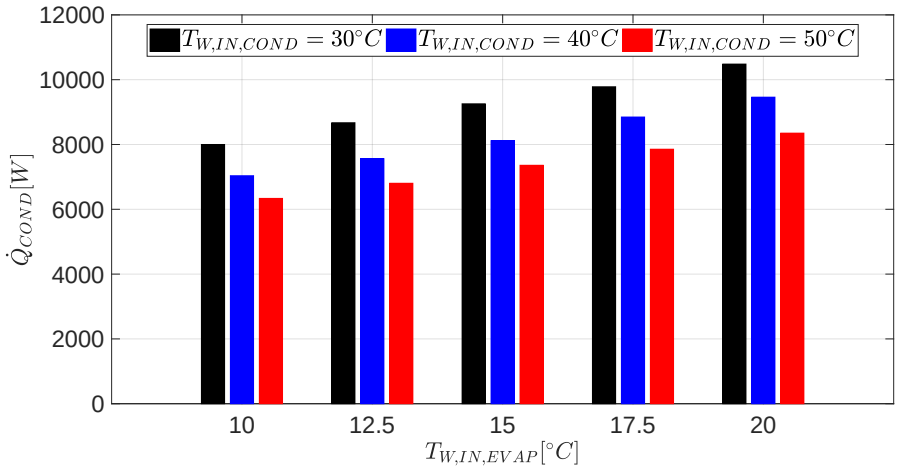

Figure 2. Condenser heating capacity as a function of evaporator water inlet temperature and for three different condenser water inlet temperature.

A similar trend is found for the COP, since it grows when the water temperature at evaporator inlet is increased (same condenser water inlet temperature) and it gets lower when the water temperature at condenser inlet increases (same evaporator water inlet temperature). This behaviour is explained remembering that the performance of any reverse cycle, the basis of a vapour compression system, is enhanced as the evaporating and the condensing temperatures get closer. As for the condenser heating capacity, when the water temperature at evaporator inlet gets higher, the evaporating temperature undergoes a strong increase, the condensing temperature a negligible one and the system performance improves. In the same way, the higher the water temperature at condenser inlet, the higher the condensing temperature, with slightly higher evaporating temperature, which leads to lower COP.

The influence of the rotational frequency of compressor shaft on condenser heating capacity and COP (group 4 in Table 3) is depicted in Fig. 4 and Fig 5 respectively. The trend of the condenser heating capacity comes from the increase of the refrigerant mass flow rate with the compressor shaft rotational frequency increase. On the other side, the COP reduces with the compressor shaft rotational frequency since the capacity increase, both at condenser and at the evaporator, under the same water inlet temperatures and flow rates leads to a lower evaporating temperature and a higher condensing temperature since the heat transfer area is constant. This, in turn, lowers the COP.

Finally, Fig. 6 shows the testing conditions inside compressor operating diagram whereas Fig. 7 reports the compressor volumetric efficiency experimentally found. From the analysis of these figures it is possible to state that the compressor was tested in a narrow range of evaporating temperatures, which is typical of water-to-water heat pump operating conditions, and that the compressor volumetric efficiency depends on the pressure ratio in a linear way, as widely discussed in technical literature [11].

4. Conclusions

In the present paper, an experimental facility for performance evaluation of pure and mixed refrigerant was presented. The facility allows to measure the most important parameters

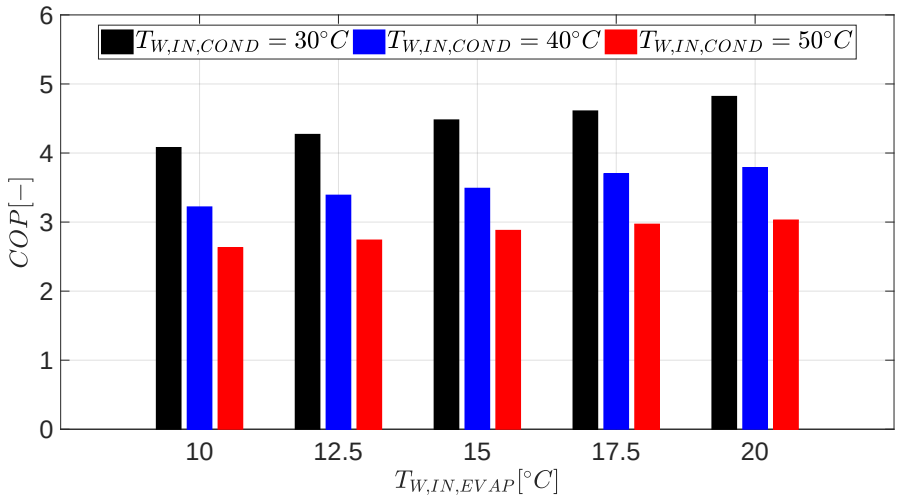

Figure 3. COP as a function of evaporator water inlet temperature and for three different condenser water inlet temperature.

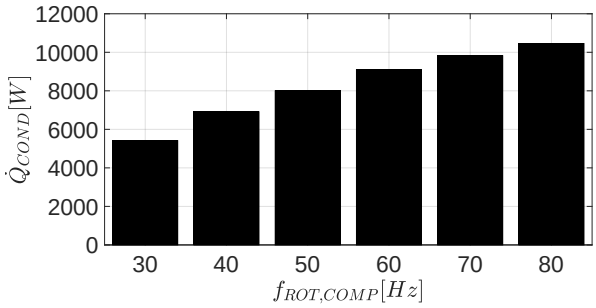

Figure 4. Condenser heating capacity vs compressor shaft rotational frequency.

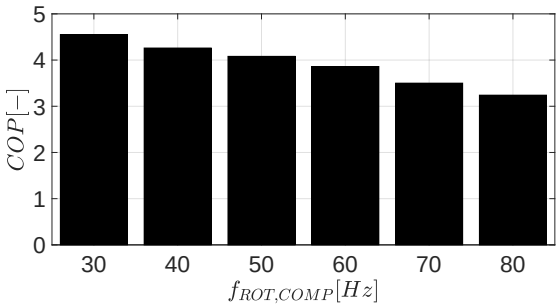

Figure 5. COP vs compressor shaft rotational frequency.

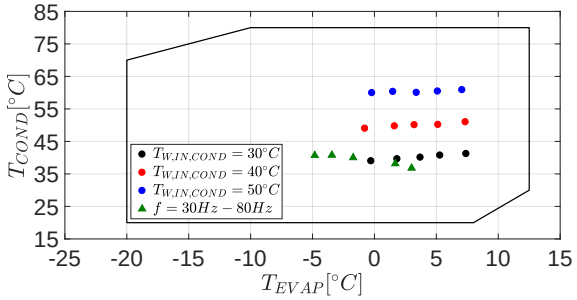

Figure 6. Representation of the testing point inside compressor operating diagram.

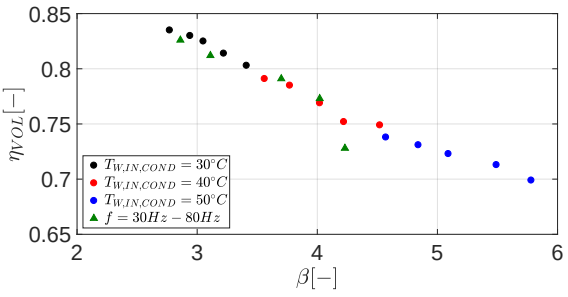

Figure 7. Compressor volumetric efficiency as a function of pressure ratio.

(pressures, temperatures, flow rates, power) for the performance characterisation of a vapour compression system under the range of operating conditions usually found in water-to-water heat pump or chillers. A variable speed reciprocating compressor is installed in the system to increase further the range of operating conditions.

First experimental campaign was aimed at introducing the most correct experimental procedure, reviewing data reduction and checking the accuracy of the results. First experimental findings show that the trends of condenser heating capacity, COP and compressor volumetric efficiency reliably agree with scientific and technical literature results.

Further studies will involve the analysis of system operation under different shaft rotational frequencies and the use of low GWP pure or mixed refrigerants.

Acknowledgments
The financial support of MIUR through the program PRIN 2015 (Grant Number 2015M8S2PA) is greatly acknowledged. Frascold company is acknowledged for providing the compressor used in the experimental campaign.

Nomenclature

c_P	Isobaric heating capacity [kJ·s^{-1}·K^{-1}]
f	Frequency [Hz]
h	Enthalpy [kJ·kg^{-1}]
$\dot{m}$	Mass flow rate [kg·s^{-1}]
$\dot{Q}$	Heat flow rate [W]
V	Volume [m^3]
$\dot{v}$	Volumetric flow rate [m^3·s^{-1}]
$\dot{W}$	Power [W]

Greek symbols

β	Pressure ratio [-]
η	Efficiency [-]
ρ	Density [kg·m^{-3}]

Subscripts

$_{ACT}$	Actual
$_{COMP}$	Compressor
$_{COND}$	Condenser
$_{IN}$	Inlet
$_{OUT}$	Outlet
$_{R}$	Refrigerant
$_{THE}$	Theoretical
$_{VOL}$	Volumetric
$_{W}$	Water

References

[1] European Union, 2014 Regulation (EU) No 517/2014 of the European Parliament and the Council of 16 April 2014 on fluorinated greenhouse gases and repealing Regulation (EC) No 842/2006. *Off. J. Eur. Union* **150** 195-230.
[2] United Nations Environment Programme, 2016 Further Amendment of the Montreal Protocol.
[3] Mota-Babiloni A., Navarro-Esbri J., Barragán Á., Molés F., Peris B. 2014 Theoretical comparison of low GWP alternatives for different refrigeration configurations taking R404A as baseline *Int. J. Refrigeration* **44** 81-90.
[4] Makhnatch P, Mota-Babiloni A., Rogstam J., Khodabandeh R. 2017 Retrofit of lower GWP alternative R449A into an existing R404A indirect supermarket refrigeration system *Int. J. Refrigeration* **76** 184-192.
[5] Pitarch M., Navarro-Peris E., Gonzálvez-Maciá J., Corberán J.M. 2017 Experimental study of a subcritical heat pump booster for sanitary hot water production using a subcooler in order to enhance the efficiency of the system with a natural refrigerant (R290) *Int. J. Refrigeration* **73** 226-234.
[6] Sánchez D., Cabello R., Llopis R., Arauzo I., Catalán-Gil J., Torrella E., 2017 Energy performance evaluation of R1234yf, R1234ze(E), R600a, R290 and R152a as low-GWP R134a alternatives *Int. J. Refrigeration* **74** 269-282.
[7] Mota-Babiloni A., Makhnatch P., Khodabandeh R., Navarro-Esbri J., 2017 Experimental assessment of R134a and its lower GWP alternative R513A *Int. J. Refrigeration* **74** 682-688.
[8] Makhnatch P., Mota-Babiloni A., Khodabandeh R., 2017 Experimental study of R450A drop-in performance in an R134a small capacity refrigeration unit *Int. J. Refrigeration* **74** 682-688.
[9] Lemmon E.W., Huber M.L. and McLinden M.O. 2013 NIST Standard Reference Database 23: Reference Fluid Thermodynamic and Transport Properties-REFPROP, Version 9.1 *National Institute of Standards and Technology, Standard Reference Data Program* Gaithersburg, MD, USA.
[10] Moffat R.J. 1988 Describing the uncertainties in experimental results *Exp. Therm. Fluid Sci.* **1** 3-17.
[11] Wang S.K. 2000 Handbook of air conditioning and refrigeration *McGraw-Hill.*